Feasibility of CO_2 capture in a mini-mill plant

A case study from the iron and steel industry

José Maria A. Pires
jose.m.pires@tecnico.ulisboa.pt

Instituto Superior Técnico, Lisboa, Portugal
Politecnico di Milano, Milano, Italia

February 2023

Abstract

Greenhouse gases, as carbon dioxide (CO_2), are one of the main drivers for global warming. Apart from the energy sector, the industrial sector, to which the iron and steel industry belongs, ranks third in the 5 greatest anthropogenic CO_2 emitting sectors. This dissertation assessed the technical and economic performance of a monoethanolamine (MEA)-based post-combustion CO_2 capture system implemented in the electric arc furnace (EAF) steel production pathway, which operates batchwise. In virtue of the developed rate-based Aspen Plus® V11 model, the best operating conditions meeting the process specifications were determined via a parametric study. In particular, it was examined the effect of the lean solvent loading, α_{LEAN}, the absorber packing height, H_{abs}, the stripper operating pressure, P_{stp}, and the stripper packing height, H_{stp}, on user-defined key performance indicators (KPI), such as the reboiler energy requirements (TER). These KPIs quantify the process performance, while simultaneously shed some light on the process requirements, thus enabling to select the best operating parameters. From all KPIs, TER was the one sought to be reduced the greatest. The optimal operating conditions were found to be equal to $\alpha_{\text{LEAN}} =$ 0.19, $H_{\text{abs}} = 32$ m, $H_{\text{stp}} = 10$ m and $P_{\text{stp}} = 2$ bara, which resulted in a TER of 3.45 GJ/t of removed CO_2, an energy saving of 36% when compared with the base case scenario. Only after the best case scenario was identified, was a flexible operation mode conceived and analysed to deal with the particularities of the EAF process. Following the process economic evaluation, the CO_2 capture costs for two scenarios (91\$/t CO_2 *vs.* 110\$/t CO_2) were compared with the current carbon tax in Portugal and the ETS permit cost. As a result, it was suggested that the CO_2 utilisation scenario is to be further analysed as it showed the lowest CO_2 removal cost. To the author's best knowledge, the simulation of such capture system applied to the EAF steelmaking process has never been described before in the literature.

Keywords: CO_2 capture, chemical absorption, MEA solvent, iron and steel industry, Aspen Plus®, batch operation

1. Introduction

1.1. Motivation

Climate change has always been a controversial topic, and not infrequently the rightful center of many discussions. Nowadays, recent data has pointed out that the Earth's global temperature has risen 0.08°C per decade since 1880, which roughly amounts to an increase of 1.01°C. In fact, nineteen of the warmest years on the record have occurred since 2000 [1].

Climate change constitutes a pressing challenge at the economic, social and environmental levels, whose long-term effects may threaten the human species' continuity on planet Earth. It is widely accepted that greenhouse gases, such as carbon dioxide, are the main responsible for this global warmth, and as such their mitigation within the various fields of activities raises increasingly greater concerns, as the global mean temperature continues to raise uncontrollably. At the United Nations Climate Change Conference in 2015, through the ratification of the Paris Agreement, the CO_2 atmospheric concentration was established to be mandatorily below 450 ppm by the year of 2100 to guarantee that the global temperature increase remains below 2°C. Following the Paris Agreement, the European Union (EU) vouched for reducing greenhouse gas emissions by 80% by 2050, and in 2019, in line with the Paris Agreement, it approved the European Green Deal with the aim of being climate-neutral by 2050 [2]. These truly ambitious energy goals set by the EU were a clear sign of acknowledgement of the urgency in addressing such challenge. Therefore, economies and, in particular, the industrial sector must undergo all kinds of transformations in order to comply with these goals. In fact, nowhere is this challenge more noticeable than in the industry, which has grown

in a consistent and rapid manner over the past few decades. Apart from the energy sector, the industrial field is among the top-3 of the greatest CO_2 emitting sectors, from which the iron and steel industry stands out, as in fig. 1. In particular, among all industries, the cement and iron and steel industries account for the biggest GHG emitters, as illustrated in the fig. 2.

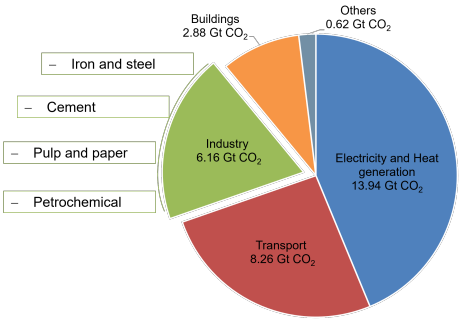

Figure 1 – Anthropogenic CO_2 emissions by source (2018). In total, 31 Gt CO_2 were globally released [3].

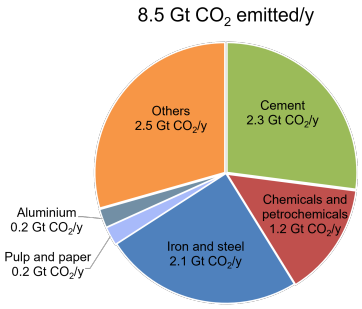

Figure 2 – CO_2 emissions by type of industry (2018) [4].

Steel, which is essentially an iron-carbon alloy with varying amounts of other alloying elements, as manganese or nickel, is undoubtedly essential to modern society and has spurred economic growth across the globe. In fact, there is not a single commodity whose importance can surpass that of steel, and the numbers speak for themselves:

- in 2021, *c.* 1.9 billion tonnes of steel were annually produced worldwide [5];
- recent forecasts predict global steel demand growth rates of 2.5 billion tonnes per *annum* by 2050 [6].

Steel is such an enabling material on many aspects. On the one hand, its combination of properties render it the material of choice for several applications: urban development, transportation, basic sanitation and water facilities all depend on steel. On the other hand, the ever-growing world's population stimulates demand for goods and services, thus burgeoning resource exploitation. Steel, as a core material, and its industry get, of course, vitalized, due to the massive importance of such material. Therefore, the iron and steel industry unsurprisingly thrives, and with it so do economies – making steel an enabling material, for that it creates opportunities for emergent economies, thus driving their development. As a result, countries get industrialized, ultimately resulting in GDP growth, but at the expense of increasing pressure on the long term sustainability of many resources and at the price of large CO_2 emissions into the atmosphere, due to the inherently energy- and carbon-intensive nature of its manufacturing process. The 2018 carbon footprint scenario shows that the iron and steel sector accounts for about 7% of all anthropogenic CO_2 emitted. In addition, with regard to the industrial sector, the iron and steel industry accounts for about 25% of the CO_2 emissions – *see* fig. 2. What is more the production of a single tonne of crude steel emits on average 1.4 tonnes of CO_2 [7], which motivates the decarbonisation of the iron and steel industry as a vital element to meet climate change mitigation targets.

2. Background

2.1. Main steelmaking production processes

As of today, there are several steel production processes. Currently, there are two dominant steel manufacturing routes:

- the blast furnace-basic oxygen furnace (BF-BOF) route, carried out at the so-called *integrated steel mill* (ISM) plants, accounts for over 70% of all produced steel. Iron is firstly produced in a blast furnace (BF), being later transformed into crude steel in a basic oxygen furnace (BOF);
- the scrap-electric arc furnace (EAF) pathway is the second largest process, accounting for 24% of the worldwide steel production. In this route, the raw material input comes mainly in the form of scrap. Secondary steelmaking plants are commonly called *mini-mills*. This work focuses on this production route.

2.2. Secondary steelmaking process overview

In the fig. 3, a simple scheme outlines the typical steelmaking process at a mini-mill. The process starts at the EAF, from which raw steel is obtained, and includes a separation system to deal with the EAF off-gas emissions. Broadly speaking, an EAF is a covered vessel set up with water-cooled walls, equipped with either one or three electrodes, some mechanical equipment and other electrical parts. The EAF operates batchwise with typical operating times of approximately one hour, even though newer EAFs can show reductions in the service time of about 30% [8]. Generally speaking, every EAF operating cycle goes through the following phases: i) charging; ii) melting; iii) refining (additions and decarburisation); iv)

slagging; and v) tapping, in which liquid raw steel is withdrawn from the furnace. The produced raw steel is then subjected to further downstream processing.

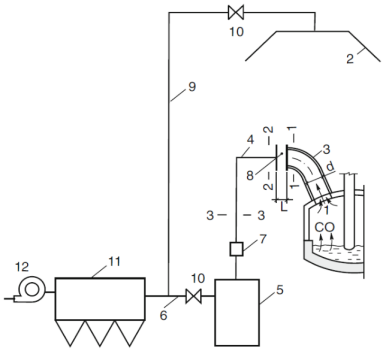

Figure 3 – EAF process overview, including the off-gas handling system [9]. 1 - opening in the furnace roof (4^{th} hole); 2 - canopy hood; 3 - roof elbow duct; 4 - stationary gas duct; 5 - drop out box; 6 - gas duct; 7 - water quenching tower; 8 - air gap; 9 - gas duct; 10 - off-gas flow rate control valve; 11 - baghouse filter; 12 - fan.

Emissions The EAF off-gas is evacuated through the so-called fourth hole, and consists mainly of carbon monoxide (CO), carbon dioxide (CO_2), nitrogen (N_2), and oxygen (O_2) [8] – even so, hydrogen (H_2) and water vapor (H_2O) may also be present as well as other organic compounds (*e.g.*, dioxins, furans) and different-sized solid particles (dusts, powders) – see table 1. This gas evacuation line is equipped with an

Table 1 – Average composition of the EAF off-gas **immediately** after exiting the 4^{th} hole [8].

	CO	CO_2	H_2	H_2O	N_2
Mole fraction (%)	20-50%	10-30%	0-40%	10-20%	20-50%

air gap, which allows atmospheric air to be mixed with the off-gas. As a consequence, the EAF off-gas gets diluted, while H_2 and CO are combusted. Even though more CO_2 is formed in that process, the overall CO_2 mole fraction in the exhaust gas plummets to around 11%.

Along the off-gas handling system, the solid-gas mixture passes through a series of coolers as well as a post-combustion chamber in order to i) reduce the amount of dioxins and furans; ii) settle coarse solid particles; and iii) complete the CO and H_2 combustion reactions. At last, the exhaust gas is sent to a baghouse filter, which captures the fine solid particles. At that stage, the EAF exhaust gas, which is clean from the solids point of view, and has no traces of CO, is then discharged as it is into the atmosphere. However, there are considerable amounts of CO_2 in the off-gas. This is, in fact, the major point source of *direct* CO_2 emissions in a mini-mill.

2.3. Absorption/stripping unit operations

Gas absorption is carried out in vertical columns, where the solvent - fed at the top of the column - and the gas mixture to be treated - that enters from the bottom - contact each other in a countercurrent pattern. As the solvent flows downwards in the column, it washes out the absorbate from the gas, and gets progressively enriched in the solute. Therefore, at the outlet of the absorber, the once *lean solvent* is now a *rich solvent* in CO_2, which is then subjected to the CO_2 stripping step. The regenerated solvent - lean solvent - flows through the *lean-rich heat exchanger* where it loses some thermal energy to the rich solvent that flows towards the stripper. After the lean-rich heat exchanger, the lean solvent is cooled down to an adequate temperature, and is re-admitted to the absorption column. Usually, there is usually a fresh amine solution make-up to compensate for solvent losses either due to solvent evaporation or irreversible chemical reactions that subtract the amount of available solvent for the separation.

In a chemical absorption plant, the desorption unit operation is the cost-determining phase, considering the energy costs. These come down to the desired degree of regeneration of the solvent at the desorber outlet. The regeneration energy requirements are the overall result of three components: i) the latent heat required to produce stripping vapor (essentially steam); ii) the sensible heat required to bring the incoming rich solution temperature to the stripper operating temperature; iii) heat required to drive desorption reactions, as in eq. (1):

$$\begin{aligned} q_{\text{reboiler}} &= q_{\text{reaction}} + q_{\text{stripping vapor}} + q_{\text{sensible}} = \\ &= \dot{n}_{\mathrm{CO_2}} \Delta H_{\text{des},\mathrm{CO_2}} + \dot{n}_{\mathrm{H_2O}} \Delta H_{\text{vap},\mathrm{H_2O}} + \\ &+ \dot{m}_{\text{solv}} \bar{c}_p (T_{in} - T_{out}) \end{aligned} \quad (1)$$

where q_{reboiler} is the reboiler heat duty (kW), q_{reaction} is the heat of reaction for CO_2 desorption (kW), $q_{\text{stripping vapor}}$ is the heat required to generate the stripping vapor (kW) and q_{sensible} is the sensible heat contribution (kW). $\dot{n}_{\mathrm{CO_2}}$ is the molar flow rate of regenerated CO_2 at the stripper (mol/s) and $\Delta H_{\text{des},\mathrm{CO_2}}$, the heat of desorption (kJ/mol). $\dot{n}_{\mathrm{H_2O}}$ is the molar flow rate of steam leaving the stripping column (mol/s) and ΔH_{vap}, the heat of vaporisation of water (kJ/mol). $\dot{m}_{\text{solv}}$ is the solvent mass flow rate (kg/s), $\bar{c}_p$, the solvent specific heat capacity (kJ/kg K) and $(T_{in} - T_{out})$ the solvent temperature difference between the stripper inlet and outlet (K).

3. Model Implementation in Aspen Plus®

3.1. Problem description

With a view to simulating a MEA-based chemical absorption CO_2 capture plant located just after the

cleaning treatment of the EAF off-gas, an Aspen Plus® rate-based steady-state model was built. Flue gas is subjected to chemical absorption treatment with a 30%wt MEA aqueous solution to promote CO_2 capture. A gas flow rate of 50 kNm^3/h and flue gas composition were assumed, based on i) the typical emissions from the EAF (*cf.* section 2); and ii) Wiley et al. [10] work - see table 2.

Table 2 – Characteristics of the fumes emitted through the EAF 4th hole.

Mini-mill plant: EAF off-gas		Wiley et al. [10] work	This work
Flow rate (Nm^3/h)		21600	50000
Pressure (bar)		1.01	1.05
Temperature (°C)		300	48
Compositions (%mol)	N_2	56	56
	H_2O	1	1
	CO_2	40	40
	O_2	3	3

It should be noted that the assumed gas composition in CO_2 is that immediately after being extracted from the EAF via the 4th hole and not that usually measured after the exhaust gas is subjected to the treatment process. In spite of such inconsistency, the absorber gas feed was preliminarily set to 40%mol in CO_2, a rather conservative approach, but necessary if the most extreme possible situation is to be assessed.

3.2. Base case simulation implementation

3.2.1 Chemical system and physical properties

The electrolyte Non-Random Two Liquid (e-NRTL) model was adopted for the thermodynamic calculations with the Redlich-Kwong (RK) extension, as suggested by [11], and in accordance with [12]. A chemistry and two reaction models were created, as follows.

Chemistry: `MEA model` This model is used as the global electrolyte calculation option and consists of the following instantaneous reactions:

$$\mathrm{MEAH^+ + H_2O \longleftrightarrow MEA + H_3O^+} \quad (2)$$
$$\mathrm{MEACOO^- + H_2O \longleftrightarrow MEA + HCO_3^-} \quad (3)$$
$$\mathrm{2\,H_2O \longleftrightarrow H_3O^+ + OH^-} \quad (4)$$
$$\mathrm{CO_2 + 2\,H_2O \longleftrightarrow HCO_3^- + H_3O^+} \quad (5)$$
$$\mathrm{HCO_3^- + H_2O \longleftrightarrow {CO_3}^{2-} + H_3O^+} \quad (6)$$

Since reactions (2)-(6) are instantaneous, only chemical equilibrium can be the sole responsible for the reaction outcome. The equilibrium constants of reactions (2)-(6) are calculated from standard free Gibbs energy change.

Reaction: `MEA-RXN` and `MEA-STP` models These two reaction models are used to represent the reactive processes within the absorber and stripper. Reactions (2), (4) and (6) also make part of the `MEA-RXN` and `MEA-STP` models, as well as the following finite rate (not instantaneous) ones:

$$\mathrm{CO_2 + OH^- \longrightarrow HCO_3^-} \quad (7)$$
$$\mathrm{HCO_3^- \longrightarrow CO_2 + OH^-} \quad (8)$$
$$\mathrm{MEA + CO_2 + H_2O \longrightarrow MEACOO^- + H_3O^+} \quad (9)$$
$$\mathrm{MEACOO^- + H_3O^+ \longrightarrow MEA + CO_2 + H_2O} \quad (10)$$

Power-law kinetics are assumed, and so rate expressions of reactions (7)-(10) share the following form:

$$r = k \exp\left(-\frac{E}{RT}\right) \prod_{i=1}^{N} (x_i \gamma_i)^{\alpha_i} \quad (11)$$

where r is the rate of reaction; k, the pre-exponential factor; T, the absolute temperature (in K); E, the activation energy (in cal/mol); R, the universal gas constant (in cal/(mol K)); x_i, the mole fraction of component i; γ_i, the activity coefficient of component i in the reaction; α_i, the stoichiometric coefficient of component i in the reaction equation and N, the number of components involved in the reaction. The aforementioned parameters were all extracted from [11]. CO_2, O_2 and N_2 were also inputted as Henry components in Aspen Plus®.

3.3. Setting the baseline steady-state case simulation

In fig. 4, the flowsheet for the base case (steady-state) simulation is shown.

3.3.1 Unit operation blocks design

Absorber A RADFRAC rate-based packed column was used to model the absorber, which operates at atmospheric pressure (1 bar). The specified rate-based model parameters and settings are shown in table 3 and table 4. The packing height totals 32 m, and corresponds to 20 stages (*i.e.*, discretization segments). Mellapak 250Y™ was the selected structured packing. Chemical reaction was incorporated in stages 1-20 through the previously defined reaction `MEA-RXN` model.

Table 3 – Selected model parameters and settings for the rate-based absorber. RCF stands for *reaction condition factor*, while FDR is the *film discretization ratio*, as per Madeddu et al. [12].

Bulk phase model			*mixed flow*
Film phase model	Film resistances	in gas film in liquid film	consider film discretize film
	Liquid film discretization	type	geometric
		RCF	0.9
		no. of points	5
		FDR	10

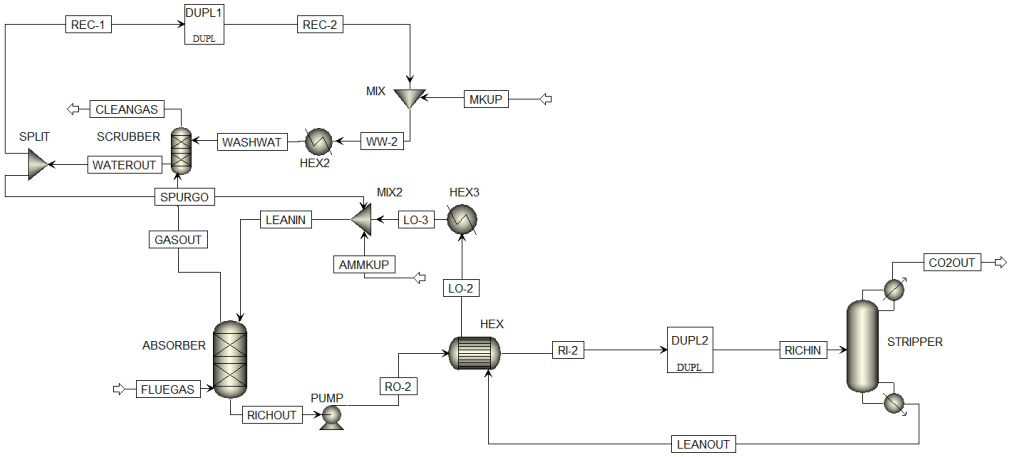

Figure 4 – Final process flowsheet regarding the baseline case steady-state simulation.

Table 4 – Selected correlations for the absorber simulation in accordance with Madeddu et al. [12] work.

	Correlations
Wetted surface area	Bravo *et al.* [13]
Material transfer coefficients	Bravo *et al.* [13]
Heat transfer coefficients	Chilton and Colburn [14]
Fractional liquid holdup	Bravo *et al.* [15]

Stripper A 12.5-m tall (total height) RADFRAC rate-based packed column was selected and discretized in 20 segments. Here, chemical reaction was incorporated into the block through the previously defined reaction `MEA-STP` model. The rate-based model settings for the stripper were the same as those for the absorber. Regarding the possible configurations for the stripper operation, it was selected the configuration in which the reflux was recycled to the stripper. A column with known feed conditions, equipped with a partial condenser and a reboiler has three degrees of freedom, which were exhausted by fixing: i) the stripper pressure at 2 bara; ii) the condenser temperature was set to 303.15 K; and iii) the CO_2 flow rate at the stripper overhead, which is equal to the removed CO_2 at the absorber, considering the global mass balance to the absorber+stripper scheme. The two last conditions were imposed by means of a block design specification as in table 5.

Table 5 – Variables specified by means of block design specifications.

Target variable	**Variable specified**	**Manipulated variable**
Condenser temperature	Stage temperature	Reflux ratio
CO_2 mass flow rate leaving top stripper	Product mass flow rate	B/F ratio

Heat Exchangers From a simulation point of view, two different types of blocks were used: i) an heater; ii) an HeatX. When modeling the lean-rich heat exchanger, the HeatX block was used, while the remaining coolers were modelled using heater blocks. A minimum temperature approach of 10 K was considered for the lean-rich heat exchanger design.

Scrubber The washing section of the absorption column is strictly modelled by a separate column (`SCRUBBER`). This strategy allows easier analysis and simulation of the washing section than when it is within the absorber. Unlike the previous cases, equilibrium was assumed in the amine scrubber. The scrubber had 10 equilibrium stages and its packing height was set to 4 m. Chemical reaction is included from stages 1-10, resorting to the reaction `MEA-RXN` model. A washing system with water recycle calls for the specification of an adequate purge fraction, which was specified as 0.1, in order to comply with the scrubber outlet clean gas specification that requires the MEA content to be equal or below to 20 mg/Nm^3.

4. Results

4.1. Baseline simulation

4.1.1 Base case simulation results

Having all the capture process equipment designed and the base case steady-state simulation running, the capture plant performance was then assessed with tailor-made key performance indicators (KPI):

- thermal energy requirements in the reboiler – *TER* – (GJ/t CO_2 removed);
- cooling water consumption in the capture process – *CWC* – (m^3 cooling water/t CO_2 removed);
- lean solvent requirements for the desired capture rate – *SR* – (m^3 solvent/t CO_2 removed).

All the considered KPIs are reported on the basis of a tonne of CO_2 removed, which helps to perform comparisons between KPIs. These were carefully chosen as

they provide a rather important insight in both capital and operating expenditures. On the one hand, both the cooling water consumption rates and the used solvent flow rate determine the size of the equipment (*i.e.*, diameter), which influences greatly the capital costs. On the other, as stated in section 2, the thermal energy requirement at the reboiler is a decisive factor in the plant operating expenditures, given the cost of steam (13 $/t [12]). The main results of the baseline case steady-state simulation are summarised in table 6.

Table 6 – Base case simulation results.

	Base case scenario
Capture rate (%)	90
Amine lean solvent loading (mol CO_2/mol MEA)	0.090
Amine rich solvent loading (mol CO_2/mol MEA)	0.532
Reboiler TER (GJ/t CO_2)	5.385
Required solvent flow rate (m^3/t CO_2)	9.94
Required cooling water (m^3/t CO_2)	770.5
at stripper condenser (m^3/t CO_2)	90.31
at lean solvent cooler (m^3/t CO_2)	656.7
at water cooler (m^3/t CO_2)	23.38
at amine scrubber (m^3/t CO_2)	0.114

After the performance of the base case capture plant at steady-state was examined, a series of parametric analyses were then carried out.

4.1.2 Parametric analyses

Parametric analyses were conducted to identify the best case regarding the plant operating conditions, based on the approach presented by Abu-Zahra et al. [16]. The following parameters were varied:

- solvent lean loading, α_{LEAN} (from 0.09 mol CO_2/mol MEA to 0.29 mol CO_2/mol MEA);
- absorber packing height, H_{abs} (from 8 m to 32 m);
- stripper packing height, H_{stp} (from 6 m to 10 m);
- stripper operating pressure, P_{stp} (from 1 bara to 2 bara).

while the effect of the variation of the abovementioned parameters on the capture process performance was once more observed recurring to the previously defined KPIs.

Effect of the lean loading and absorber packing height on the KPIs In fig. 5, the reboiler thermal energy requirement and the (lean) solvent requirement are plotted against different lean solvent loadings for the absorber packing heights of 8, 16, 24 and 32 m. The lean solvent loading indicates to what extent was the solvent regenerated in the stripper. According to Abu-Zahra et al. [16], the optimum lean solvent loading can be recognized by spotting the point at which the reboiler TER is the lowest. Thus, α_{LEAN} was varied until the solvent loading for which the reboiler TER is minimal was found out.

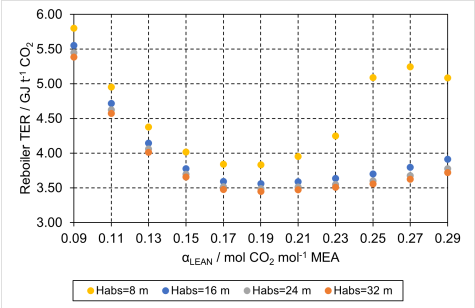

(a) Reboiler thermal energy requirements at various solvent lean loadings (0.09 to 0.29 mol CO_2/mol MEA) for different absorber packing heights, for a capture rate of 90%.

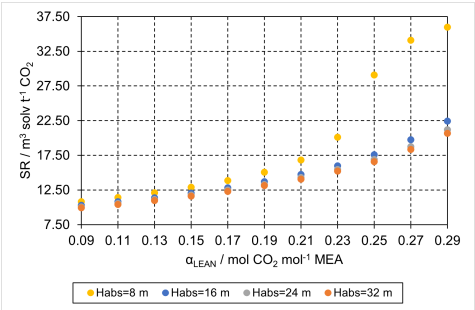

(b) Volumetric quantity of solvent required per tonne of removed CO_2 at several lean solvent loadings (0.09 to 0.29 mol CO_2/mol MEA) for different absorber packing heights, for a capture rate of 90%.

Figure 5 – Effect of the α_{LEAN} on two of the studied KPIs.

When analysing the TER *vs.* α_{LEAN} plot, as fig. 5(a), recall the three components in which the reboiler TER can be decomposed – *cf.* section 2. Changing the degree of regeneration will directly affect the performance of the absorber. Begin by considering a given H_{abs}. On the one hand, for low α_{LEAN}, reboiler TER quickly escalates, due to the abrupt increase in the amount of stripping steam needed to originate such poor solvent composition in CO_2 at the stripper outlet, but, on the other hand, the required solvent flow rates that ensure the 90% capture rate at the absorber are also quite reduced, given the increased solvent absorption capacity, as shown in fig. 5(b). However, it is not feasible to regenerate the solvent to that great extent, because high regeneration levels consume great amounts of stripping vapor. On the other hand, as α_{LEAN} gets higher, the solvent circulation flow rate will have to vary in accordance with these changes in the degree of regeneration, if the CO_2 capture rate is to be maintained. For this

reason, reboiler TER rises quickly (although not as sharply as it did for low lean solvent loadings) on account of the higher solvent circulation flow rates – see fig. 5(b), where, for $H_{\text{abs}} = 24$ m, the lean solvent consumption increased fourfold within the range of the considered α_{LEAN}. Now, the observed reboiler TER is due to the rich solvent heat up as it enters the stripper.

Therefore, as the TER *vs.* α_{LEAN} curve is flanked by two relative maxima, a minimum TER should be expected in between, which indeed shows up, as in fig. 5(a). This is consistent with the works reported by Abu-Zahra et al. [16]. As such, in this work, α_{LEAN} = 0.19 mol CO_2/mol MEA is identified as the optimal lean solvent loading, being also the optimal α_{LEAN} for all the absorber packing heights considered.

In addition, it was observed that higher reboiler TER are achieved with smaller H_{abs}, as fig. 5(a) shows. Reducing the base case H_{abs} in -75% entails a TER increase of 11%. Whenever the packing height enlarges, the contact area increases, resulting in increased absorption capacity.

Regarding the remaining performance indicator - CWC -, note that process water is used in four different equipment: i) at the stripper condenser; ii) at the lean cooler after the lean-rich heat exchanger; iii) at the MEA scrubber; iv) at the washing water cooler. For this reason, the results exhibited in fig. 6 are the outcome of the influence of these four contributions. For all the absorber packing heights evaluated, the lean cooler water requirements account for around 86% of all CW requirements. As a result, the global profile of the CWC *vs.* α_{LEAN} follows the lean cooler process water requirements behaviour. Put differently, the lean cooler water demand is dominant compared with the remaining components.

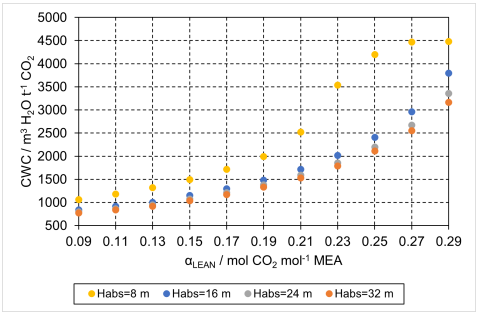

Figure 6 – Cooling water requirements at various lean solvent loadings (0.09 to 0.29 mol CO_2/mol MEA) for different absorber packing height, for a capture rate of 90%.

For low α_{LEAN}, smaller solvent flow rates are needed to achieve the desired 90% capture rate than compared with higher lean solvent loadings. As smaller flow rates are to be handled in the lean cooler, the cooler duty reduces, thus diminishing the CWC. The opposite effect is noticed for high α_{LEAN}, resulting on the observations depicted in fig. 6.

Effect of the stripper operating pressure on the KPIs

Stripper operating conditions play a major role in the success of the desorption task. Thus, the effect of different temperature and pressure conditions was examined, whose results are shown in fig. 7. The kettle-type reboiler operates with low pressure (LP) steam at 144°C, coming, for instance, from an utility plant installed at the industrial facility.

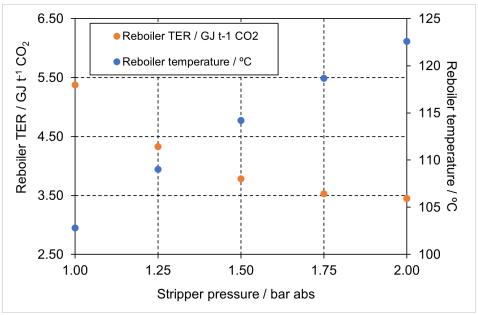

Figure 7 – Reboiler TER and reboiler temperature for different stripper operating pressures.

High stripper pressures help reduce quite substantially the reboiler TER in about 36%, as shown in fig. 7. As the stripper operating pressure changes, the reboiler temperature changes accordingly, so that increasing reboiler temperatures decrease the ratio of the water partial pressure to the CO_2 vapor pressure, $p_{\text{H}_2\text{O}}/p_{\text{CO}_2}$, owing to: i) the CO_2 vapor pressure, $p^{sat}_{\text{CO}_2}(T)$, which increases more rapidly with temperature changes than the H_2O vapor pressure, $p^{sat}_{\text{H}_2\text{O}}(T)$, according to the Clausius-Clapeyron equation (since the heat of absorption of CO_2 is almost twice the heat of vaporization of H_2O). At greater-than-the-atmospheric stripper working pressures, the stripper operates at higher temperatures, resulting in a CO_2 vapor pressure increase. As a consequence, so does the driving force for CO_2 stripping, ultimately leading to higher CO_2 mass transfer rates; ii) as the CO_2 stripping reactions are endothermic, benefit with higher temperatures. Both these two effects result on a easier desorption task; and iii) at higher pressures, water boils at a higher temperatures. This means that elevating the stripper pressure to values greater-than-the-atmospheric suppresses water vaporisation. Overall, these effects culminate in a lower reboiler TER as the P_{stp} is raised. In addition, as P_{stp} went for 1 bara to 2 bara, the LP steam flow rates reduced in about 36%, in line with the reduced reboiler TERs.

The influence of the P_{stp} on the other two defined KPIs is shown in fig. 8. It was found that the stripper pressure had no influence on the solvent requirements. This fact comes as no surprise as the solvent requirements are mainly set by the absorber operation. On the other hand, greater stripper working pressures reduce the CWC. In particular, greater pressures imply cuts of the order of 49% in the amount of cooling water employed in the condenser.

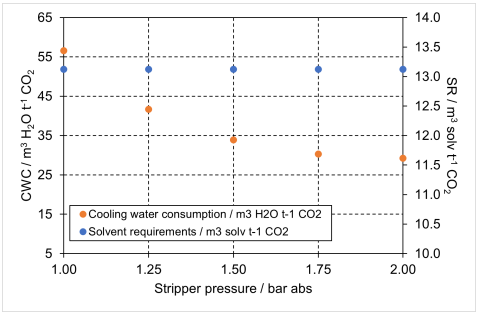

Figure 8 – Effect of stripper working pressure on the CW and SR KPIs.

4.1.3 Final considerations

Whether it is for economic or sustainable reasons, the smaller the process requirements the better. For this reason, the operating parameters that ensure the lowest possible process requirements should be sought.

Table 7 – Comparison between the base case simulation results and those of the identified best case.

	Scenarios	
	Base case	**Best case**
Capture rate (%)	90%	
Amine lean solvent loading (mol CO_2/mol MEA)	0.090	0.190
Amine rich solvent loading (mol CO_2/mol MEA)	0.532	0.525
Reboiler TER (GJ/t CO_2)	5.385	3.449
Required solvent flow rate (m^3/t CO_2)	9.94	13.1
Required cooling water (m^3/t CO_2)	770.5	1331
at stripper condenser (m^3/t CO_2)	90.31	48.39
at lean solvent cooler (m^3/t CO_2)	656.7	1272
at water cooler (m^3/t CO_2)	23.38	10.56
at amine scrubber (m^3/t CO_2)	0.114	0.053

Delving into the results shown in table 7, it can be observed that the best case outperforms the baseline one only in the reboiler TER, which is undoubtedly the most important factor to consider when selecting the best operating conditions. Its effect on the operating expenditures outweighs the effect of the SR and CWC on the process economics. The reasons for such claim revolve around the cost of steam. In effect, increasing the lean solvent loading from 0.09 to 0.19 achieves a 36% reduction in TER, which is beneficial in terms of energy efficiency. As for the remaining performance criteria, the baseline case scenario globally shows smaller solvent and process water consumption rates than the best case scenario found. Notwithstanding, for the latter KPI, a careful inspection of the results reveals otherwise. That is, all but one process water requirements diminish as α_{LEAN} increases. However, these reductions are completely overshadowed, since the lean cooler water requirements dominate over the other components. In relation to the former KPI, there is a trade-off between lower reboiler TERs and lower SRs, as it is impossible to simultaneously satisfy both, since greater α_{LEAN} require higher amounts of solvent if the capture rate is to remain unchanged.

4.2. Flexible operation mode

After the best case scenario was identified, a flexible operation mode needed to be suggested and discussed, since the EAF emits fumes in an intermittent way, which denotes a transient process, and is not consistent with the laid out steady-state simulation. The final process operation should be as that depicted in fig. 9. Recall that, during an EAF working cycle, there is a portion of time during which no fumes are exhausted. Therefore, the CO_2 capture plant must operate in a flexible way. Within the scope of this work, it is suggested that the following operation mode be adopted for every working cycle:

- during the time in which the EAF is operating, the EAF fumes arrive at the absorber, where CO_2 is absorbed into the MEA-based solvent. The required solvent flow rate that ensures the desired capture rate is provided. The newly-rich solvent goes to the rich solvent tank, and from there to the regeneration section;

- during the time in which the EAF is not operating: atmospheric air should be made to pass through the absorber in order to ensure correct continuous operation of the absorption unit. Whether fumes evolve from the EAF or not, atmospheric air is always admitted to the process right after the EAF fourth gap. As the lean solvent flowing through the column will not absorb CO_2, it is recycled to the absorber.

Regeneration is allowed to take place during the entire operation cycle. Freshly regenerated solvent is directed to the lean solvent tank.

4.3. Project economic evaluation

At last, an economic evaluation of this project was entirely carried out resorting to the Aspen Process Economic Analyser® (APEA), based on USD for the first quarter of 2018. Two scenarios were investigated: scenario I considered CO_2 is used as feedstock for an urea production facility; while, scenario II assumes the removed CO_2 is to be compressed and stored into a geological formation. The main assumptions for this economic evaluation are summarized in table 8.

Capital costs must be annualized, so that all costs are referred to the same time base. To that purpose, these costs were converted into a series of annual payments (annuity) for every year of project life. Hence, the total plant annual cost is given by eq. (12):

$$TAC = AFCI + OC = FCI\frac{(1+i)^n\ i}{(1+i)^n - 1} + OC \tag{12}$$

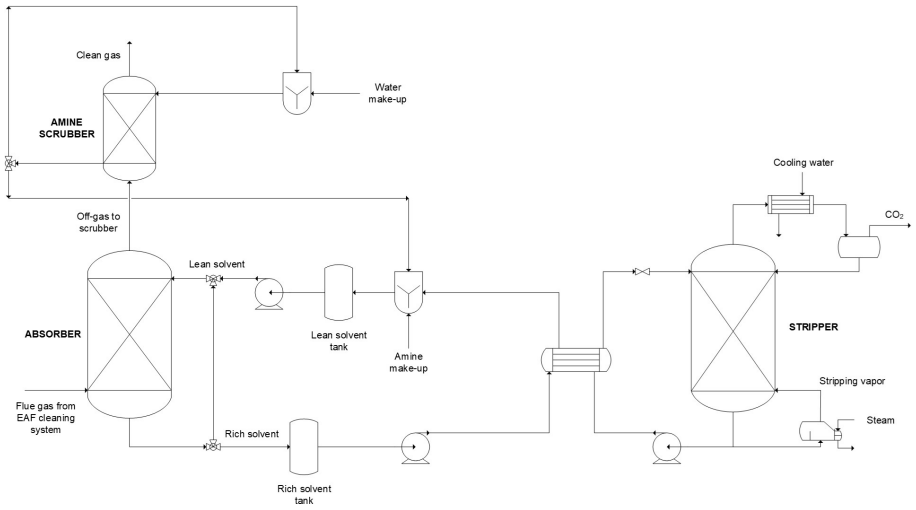

Figure 9 – Final flowsheet for the simulated process under flexible operation.

Table 8 – Economic evaluation assumptions.

Present value	USD 2022
Plant operating period	8000 h/year
Project economic life	30 years [17]
Interest rate	8% [17]
Tax rate	40%
Salvage value	20% of capital costs
Depreciation method	Straight-line method
% Working capital	5% of total capital investment
Labour cost	20$/operator/h
Supervisor cost	35$/operator/h
Operating charges	25% of operating labor
Plant overhead cost	50% of operating labor and maintenance
General and Administrative expenses	8% of total direct production costs

where TAC stands for total annual costs, $AFCI$ is the annualized fixed-capital investment, FCI stands for the fixed-capital investment, OC for operating expenditures, n the expected project life, and i, the discount rate. In table 9, the total plant costs are breakdown into the annualized capital expenditures and operating ones. The CO_2 removal cost is also showcased.

Table 9 – Total plant costs and CO_2 capture costs for both scenarios.

CRF = 8.9%	**Scenario I**	**Scenario II**
Annualized capital costs (M$/y)	2.714	4.304
Operating costs (M$/y)	25.61	29.64
Total plant costs - TAC (M$/y)	**28.33**	**33.94**
CO_2 avoided (Mt CO_2/y)	0.310	0.310
CO_2 capture cost ($/t CO_2)	**91.39**	**109.5**

It is quite interesting to compare the CO_2 capture cost with the current carbon tax, since if it were not for the raising environmental concerns, CO_2 would not be removed, as CO_2 capture projects are generally not economically attractive, considering the high involved plant costs – see table 10.

Table 10 – Comparison between the CO_2 capture cost and the carbon tax and ETS permits in force.

	Scenario I	**Scenario II**
Carbon tax ($/t CO_2eq)	25.40	
Cost of ETS certificate ($/t CO_2eq)	93.42	
CO_2 removal cost ($/t CO_2)	91.39	109.5

Taking into consideration the results of table 10, scenario I is less expensive than scenario II, considering from the outset the additional equipment needed in the compression line. Furthermore, cost estimation for scenario II was not comprehensive of the transport or storage costs, which would certainly increase further costs. On the other hand, scenario I promotes circular economy as the sub-products of an industry are the raw materials of another one. On the other hand, it is difficult to establish a solid comparison between the attained CO_2 capture costs with others obtained for other mini-mill plants, as to the author's best knowledge little or none cost estimation reports for the application of carbon capture to mini-mills have been described in the literature. Looking at the capture costs for both scenarios, and confronting with the carbon tax, it would seem from the profitability point of view that implementing a CO_2 capture system would not be feasible, as the current carbon tax in Portugal is substantially smaller than the cost of removal for both scenarios. However, different countries enforce more or less tighter environment policies, ultimately meaning that there is quite some variability on these charges, depending on the plant location. In fact, if this plant were to be installed in Sweden, it would be subject to a stricter carbon tax - *cf.* 25.40$/t CO_2 in Portugal *vs.* 124.61$/t CO_2 in Sweden. On the other hand, regarding the ETS permits, it could be argued that it would be economically favourable to pay just for

enough allowances such that the uncovered emissions by the free allowances are then covered, rather than investing in a CO_2 capture project. However, ETS free allowances will decrease over time, until a situation of all emitted CO_2 is to be charged, which means companies are necessarily forced to reduce CO_2 emissions in the long term, as environment policies are getting stricter as time goes by. Having that said, comparing the obtained CO_2 removal costs in this work and the ETS permits cost, the choice for implementing such solution is clear as the capture costs for both scenarios and the current ETS costs are quite competitive with each other. Therefore, scenario I is recommended for further analysis, as it shows a slightly lower capture cost than that of scenario II.

5. Conclusions

In light of the growing GHG emissions by the industrial sector to which the iron and steel industry belongs, this dissertation successfully proposed the application of CO_2 capture via chemical absorption to a mini-mill plant, even if at a conceptual stage. To the author's best knowledge, there are no references in the literature to an Aspen Plus® simulation of a chemical absorption plant installed in the EAF exhaust gas system. The rate-based model developed, due to its rigor, can be used as a guide for CO_2 absorption processes using MEA solvent. Furthermore, this work aimed at finding the best working conditions for the operation of that carbon capture system applied to a mini-mill. To that purpose, a series of parametric analysis were carried out, which revealed that the optimal operating conditions were found to be equal to $\alpha_{\text{LEAN}} = 0.19$, $H_{\text{abs}} = 32$ m, $H_{\text{stp}} = 10$ m and $P_{\text{stp}} = 2$ bara, which resulted in a TER of 3.45 GJ/t of removed CO_2. Due to the strict regulation in force for MEA emissions into the atmosphere, a washing section was designed, and a purge fraction equal to 0.1 was selected. Only after the steady-state best operating conditions were identified could the flexible operating mode be laid out, which exploited the dedicated air gap for CO post-combustion. Lastly, an economic evaluation of this project was carried out, in which both CCS and CCU scenarios were considered. The CO_2 capture total cost for the CCU scenario was smaller than that for the CCS scenario – 91.39 \$/t CO_2 captured *vs.* 109.5 \$/t CO_2 captured, respectively. For this reason, the CCU scenario is recommended for further analysis. In any case, the obtained values if compared with the increasing cost of the ETS certificates may compel decision-makers regarding the consideration of such solution applied to mini-mill plants, thus contributing for a healthier planet Earth. In the near future, the most immediate point to develop would be a further analysis of the CCU scenario, considering this time a flue gas consisting of 11%mol CO_2, which would correspond to the actual process conditions. Furthermore, other process configurations such as the absorber intercooler or the rich-split process could also be simulated in Aspen Plus® to examine their benefits on the studied process.

References

[1] National Aeronautics and Space Administration. Global Climate Change, Vital Signs of the Planet. https://climate.nasa.gov, 2022. [Online; accessed 5 April 2022].

[2] Monica Draxler et al. Greensteel for Europe: Technology assessment and roadmapping. https://ec.europa.eu/clima/eu-action/climate-strategies-targets/2050-long-term-strategy_en, March 2021. [Online; accessed 21 April 2022].

[3] IEA. Global CO_2 emissions by sector. https://www.iea.org/data-and-statistics/charts/global-co2-emissions-by-sector-2018, 2018. [Online; accessed 07 April 2022].

[4] IEA. Tracking Industry 2020. https://www.iea.org/reports/tracking-industry-2020, 2020. [Online; accessed 07 April 2022].

[5] EUROFER. European Steel in figures 2022 - data covering 2021. https://www.eurofer.eu/publications/brochures-booklets-and-factsheets/european-steel-in-figures-2022/, 2022. [Online; accessed 07 August 2022].

[6] *Steeling demand: mobilising buyers to bring net-zero steel to market before 2030*. Material Economics and Energy Transitions Commission, July 2021.

[7] *Industrial Transformation 2050—Pathways to Net-Zero Emissions from EU Heavy Industry*. Material Economics, 2019.

[8] Maria Elena Fabiani. *Recupero energetico dagli off-gas dei forni elettrici ad arco tradizionali. Applicazione di un procedimento innovativo con materiali a cambiamento di fase*. PhD thesis, Università degli Studi di Udine, 2012. URL https://core.ac.uk/download/pdf/158819635.pdf.

[9] Marcus Kirschen et al. Off-gas measurements at the EAF primary dedusting system. *EEC*, 2005.

[10] Dianne E Wiley, Minh T Ho, and Andrea Bustamante. Assessment of opportunities for CO_2 capture at iron and steel mills: an Australian perspective. *Energy Procedia*, 4:2654–2661, 2011.

[11] Aspen Technology Inc. *Rate-based model of the CO_2 capture process by MEA using Aspen Plus*. Burlington (USA), 2014.

[12] Claudio Madeddu, Massimiliano Errico, and Roberto Baratti. *CO_2 Capture by Reactive Absorption-Stripping: Modeling, Analysis and Design*. Springer, 2018.

[13] Jose L Bravo, J Antonio Rocha, and JR Fair. Mass transfer in gauze packings. *Hydrocarbon processing (International ed.)*, 64 (1):91–95, 1985.

[14] Thomas H Chilton and Allan Philip Colburn. Mass transfer (absorption) coefficients prediction from data on heat transfer and fluid friction. *Industrial & engineering chemistry*, 26(11):1183–1187, 1934.

[15] JL Bravo, JA Rocha, and JR Fair. A comprehensive model in the performance of columns containing structured packings, distillation and absorption, institution of chemical engineers symposium series 128. *Inst Chem Eng*, 1:PA48–A507, 1992.

[16] Mohammad RM Abu-Zahra et al. CO_2 capture from power plants: Part I. A parametric study of the technical performance based on monoethanolamine. *International Journal of Greenhouse gas control*, 1(1):37–46, 2007.

[17] Kangkang Li, Wardhaugh Leigh, Paul Feron, Hai Yu, and Moses Tade. Systematic study of aqueous monoethanolamine (MEA)-based CO_2 capture process: Techno-economic assessment of the MEA process and its improvements. *Applied Energy*, 165:648–659, 2016.